DALTON

Structural and electronic impact of fluorine in the *ortho* positions of the phenoxy groups of phenyl-phosphonite and -phosphinite ligands in compounds of platinum-group metals

Malcolm J. Atherton,[a] John Fawcett,[b] Adrian P. Hill,[b] John H. Holloway,[b] Eric G. Hope,[b] David R. Russell,[b] Graham C. Saunders *,[b] and Russell M. J. Stead[b]

[a] *BNFL Fluorochemicals Ltd., Springfields, Salwick, Preston PR4 0XJ, UK*
[b] *Department of Chemistry, University of Leicester, Leicester LE1 7RH, UK*

The phosphonites $PPh(OPh)_2$ **I** and $PPh(OC_6H_3F_2\text{-}2,6)_2$ **II**, and the phosphinites $PPh_2(OPh)$ **III** and $PPh_2(OC_6H_3F_2\text{-}2,6)$ **IV** reacted with $[\{RhCl(\mu\text{-}Cl)(\eta^5\text{-}C_5Me_5)\}_2]$ to yield the complexes $[RhCl_2L(\eta^5\text{-}C_5Me_5)]$ [L = $PPh(OPh)_2$ **1**, $PPh(OC_6H_3F_2\text{-}2,6)_2$ **2**, $PPh_2(OPh)$ **3** or $PPh_2(OC_6H_3F_2\text{-}2,6)$ **4**]. The perprotio-phosphonite and -phosphinite, **I** and **III**, reacted with $[\{PtCl(\mu\text{-}Cl)(PEt_3)\}_2]$ to yield exclusively the *cis* isomers of $[PtCl_2(PEt_3)\{PPh(OPh)_2\}]$ **5** and $[PtCl_2(PEt_3)\{PPh_2(OPh)\}]$ **7**. The fluorine-containing phosphonite and phosphinite, **II** and **IV**, reacted with $[\{PtCl(\mu\text{-}Cl)(PEt_3)\}_2]$ to give the *trans* isomers of $[PtCl_2(PEt_3)\{PPh(OC_6H_3F_2\text{-}2,6)_2\}]$ **6a** and $[PtCl_2(PEt_3)\{PPh_2(OC_6H_3F_2\text{-}2,6)\}]$ **8a**, which isomerize slowly in acetone solution to yield the *cis* isomers **6b** and **8b**. Values of ^1J(RhP) and ^1J(PtP) strongly suggest that the presence of fluorine atoms in the *ortho* positions of the phenoxy groups has a negligible effect on the electronic properties of the phosphorus atoms of these ligands. X-Ray single-crystal structural studies on **1**, **4**, **6a**, **6b**, **7**, **8a** and **8b** revealed that the fluorine atoms do, however, exert a profound steric influence.

The presence of fluorine in strategic positions in phosphorus(III) ligands can have a dramatic impact on the nature of the complexes they form. Transition-metal complexes of $P(C_6F_5)_3$,[1–3] $P(C_6H_3F_2\text{-}2,6)_3$,[4] $PPh(C_6F_5)_2$,[2] $PPh_2(C_6F_5)$,[2,5] $PPh_2(C_6H_3F_2\text{-}2,6)_3$[4] and $(C_6F_5)_2PCH_2CH_2P(C_6F_5)_2$[2,6–10] possess significantly different chemical and structural properties to their perprotio analogues. These differences are ascribed to the σ-withdrawing property of the fluorine atom and its greater bulk compared to that of the hydrogen atom, and it is apparent that the fluorine atoms in the *ortho* positions of the phenyl rings exert the largest steric and electronic effects.[4] We are interested in the effects that fluorine in the *ortho* positions of aryl rings in other phosphorus(III) ligands bestow upon transition-metal complexes. We have reported the preparation and characterization of the fluorine-containing tris(2,6-difluorophenyl) phosphite and its complexation with platinum-group metals.[11–13] Comparison of the NMR spectral data for this compound and its complexes with those of triphenyl phosphite and its complexes suggests that the two ligands possess similar σ-donor/π-acceptor properties. The crystal structures of $[IrCl_2\{P(OC_6H_3F_2\text{-}2,6)_3\}(\eta^5\text{-}C_5Me_5)]$[11] and *trans*-$[PtCl_2(PEt_3)\{P(OC_6H_3F_2\text{-}2,6)_3\}]$[12,13] indicate that tris(2,6-difluorophenyl) phosphite is considerably more bulky than triphenyl phosphite and this has a dramatic effect on its complexes. Here we report the new fluorine-containing phosphorus compounds bis(2,6-difluorophenyl) phenylphosphonite and (2,6-difluorophenyl) diphenylphosphinite and compare their electronic and steric effects with those of $PPh(OPh)_2$[14] and $PPh_2(OPh)$[15] by NMR and X-ray crystallographic studies of the rhodium and platinum complexes, $[RhCl_2L(\eta^5\text{-}C_5Me_5)]$ and $[PtCl_2(PEt_3)L]$.

Results and Discussion

Synthesis and characterization of the compounds

Treatment of $PPhCl_2$ and PPh_2Cl with 2,6-difluorophenol in the presence of triethylamine yielded bis(2,6-difluorophenyl) phenylphosphonite **II** and 2,6-difluorophenyl diphenylphosphinite **IV**, respectively (Scheme 1). They were both obtained

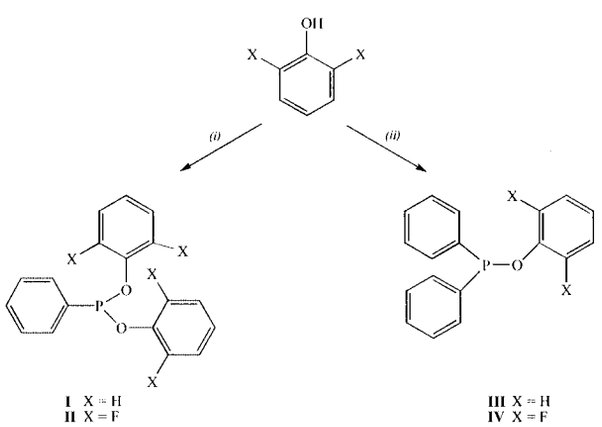

Scheme 1 (*i*) $PPhCl_2$, NEt_3, Et_2O, 0 °C; (*ii*) PPh_2Cl, NEt_3, Et_2O, 0 °C

as yellow oils in *ca.* 50% yields, and were characterized by mass, NMR and IR spectroscopies. The known compounds $PPh(OPh)_2$ **I**[14] and $PPh_2(OPh)$ **III**[15] were prepared similarly. The $^{31}P\text{-}\{^1H\}$ NMR spectrum of **II** exhibits a quintet at δ 183.5, compared with 158.5 for **I**, with a coupling constant, ^4J(PF), of 32.9 Hz, and **IV** exhibits a triplet at δ 133.1, compared with 111.1 for **III**, with ^4J(PF) 28.5 Hz. The values of δ_P for the compounds $P(OPh)_3$ (128.2), $P(OC_6H_3F_2\text{-}2,6)_3$ (131.8),[11] **I**–**IV** and PPh_3 do not follow a simple trend. Values for three-co-ordinate phosphorus(III) compounds vary considerably and, although that for PR_3 may be dependent upon the electronegativity of R and the R–P–R angles, those for P–O–R compounds do not show such a simple dependence.[16] Thus, the electronic nature of the phosphorus in these compounds cannot be discerned from the values of δ_P. It is noted, however, that whilst the values of δ_P for $P(OPh)_3$ and $P(OC_6H_3F_2\text{-}2,6)_3$ are similar, the differences between those for **I** and **II**, and for **III** and **IV**, are 22–25 ppm, with δ_P for the fluorine-containing compounds at higher frequency than those of the respective perprotio analogues. The values of the coupling constants ^4J(PF)

Table 1 Analytical, mass and ^{1}H NMR spectral data for compounds **1**–**8**

Compound	Analysis (%)[a] and *m*/*z*[b]	^{1}H NMR (δ, *J*/Hz)
1	C, 55.5 (55.7); H, 4.9 (5.0); Cl, 12.35 (11.75) 602 (M^+), 567 ([M − Cl]$^+$), 531 ([M − 2Cl − H]$^+$)	8.16 (2 H, m, PPh), 7.28 (7 H, m, PPh and *o*-H of OC_6H_5), 7.22 (4 H, vt, *J* 7.9, *m*-H of OC_6H_5), 7.05 [2 H, t, $^3J(H_mH_p)$ 7.0, *p*-H of OC_6H_5], 1.47 [15 H, d, *J*(PH) 4.9, CH_3][c]
2[d]	C, 48.3 (48.3); H, 3.8 (3.8); Cl, 13.0 (13.4) 674 (M^+), 639 ([M − Cl]$^+$)	8.08 (2 H, m, PPh), 7.41 (3 H, m, PPh), 6.98 (2 H, m, *p*-H of $OC_6H_3F_2$), 6.63 (4 H, m, *m*-H of $OC_6H_3F_2$), 5.32 (s, CH_2Cl_2), 1.56 [15 H, d, *J*(PH) 4.9, CH_3][c]
3[e]	C, 56.4 (56.0); H, 5.0 (5.0); Cl, 15.45 (14.5) 586 (M^+), 551 ([M − Cl]$^+$), 515 ([M − 2Cl − H]$^+$)	8.21 (4 H, m, PPh), 7.45 [2 H, d, $^3J(H_oH_m)$ 7.1, *o*-H of OC_6H_5], 7.36 (6 H, m, PPh), 7.23 (2 H, vt, *J* 7.5, *m*-H of OC_6H_5), 7.00 [1 H, t, $^3J(H_mH_p)$ 7.3, *p*-H of OC_6H_5], 5.30 (s, CH_2Cl_2), 1.36 [15 H, d, *J*(PH) 3.9, CH_3][c]
4	C, 53.2 (54.0); H, 4.4 (4.5); Cl, 11.15 (11.4) 622 (M^+), 587 ([M − Cl]$^+$)	8.12 (4 H, m, PPh), 7.39 (6 H, m, PPh), 6.86 (1 H, m, *p*-H of $OC_6H_3F_2$), 6.72 (2 H, vt, *J* 8.1, *m*-H of $OC_6H_3F_2$), 1.42 [15 H, d, *J*(PH) 4.0, CH_3][c]
5[f]	C, 44.0 (42.5); H, 4.1 (4.5); Cl, 10.4 (10.45) 643 ([M − Cl]$^+$), 605 ([M − 2Cl − 3H]$^+$)	7.31 (15 H, m, PPh and OC_6H_5), 2.11 (6 H, m, CH_2), 1.02 [9 H, dt, ^3J(PH) 17.8, ^3J(HH) 7.6, CH_3][c]
6a	750 (M^+), 715 ([M − Cl]$^+$)	8.02 (2 H, m, PPh), 7.52 (3 H, m, PPh), 7.18 (2 H, m, *p*-H of $OC_6H_3F_2$), 7.02 (4 H, vt, *J* 8.0, *m*-H of $OC_6H_3F_2$), 1.84 (6 H, m, CH_2), 1.08 [9 H, dt, ^3J(PH) 16.9, ^3J(HH) 7.6, CH_3][g]
6b	C, 38.1 (38.4); H, 3.3 (3.5); Cl, 9.2 (9.45) 750 (M^+), 715 ([M − Cl]$^+$)	7.92 (2 H, m, PPh), 7.56 (1 H, m, *p*-H of PPh), 7.46 (2 H, m, PPh), 7.26 (2 H, m, *p*-H of $OC_6H_3F_2$), 7.04 (4 H, m, *m*-H of $OC_6H_3F_2$), 2.33 (6 H, m, CH_2), 1.28 [9 H, dt, ^3J(PH) 17.7, ^3J(HH) 7.6, CH_3][g] 7.91 (2 H, m, PPh), 7.47 (1 H, m, PPh), 7.36 (2 H, m, PPh), 7.07 (2 H, m, *p*-H of $OC_6H_3F_2$), 6.67 (4 H, m, *m*-H of $OC_6H_3F_2$), 2.28 (6 H, m, CH_2), 1.27 [9 H, dt, ^3J(PH) 17.8, ^3J(HH) 7.6, CH_3][c]
7	C, 43.0 (43.5); H, 4.2 (4.6); Cl, 9.9 (10.7) 662 (M^+), 627 ([M − Cl]$^+$), 590 ([M − 2Cl − 2H]$^+$)	7.66 (4 H, m, PPh), 7.44 (6 H, m, PPh), 7.18 (2 H, vt, *J* 7.6, *m*-H of OC_6H_5), 7.07 [1 H, t, $^3J(H_mH_p)$ 6.9, *p*-H of OC_6H_5], 6.94 [2 H, d, $^3J(H_oH_m)$ 7.6, *o*-H of OC_6H_5], 2.08 (6 H, m, CH_2), 1.09 [9 H, dt, ^3J(PH) 17.6, ^3J(HH) 7.7, CH_3][c]
8a	698 (M^+), 663 ([M − Cl]$^+$)	7.87 (4 H, m, PPh), 7.51 (6 H, m, PPh), 7.14 (1 H, m, *p*-H of $OC_6H_3F_2$), 6.99 (2 H, vt, *J* 8.3, *m*-H of $OC_6H_3F_2$), 1.87 (6 H, m, CH_2), 1.12 [9 H, dt, ^3J(PH) 16.7, ^3J(HH) 7.6, CH_3][g]
8b	C, 40.9 (41.3); H, 4.0 (4.0); Cl, 10.6 (10.15) 698 (M^+), 663 ([M − Cl]$^+$)	7.92 (4 H, m, PPh), 7.48 (6 H, m, PPh), 7.08 (1 H, m, *p*-H of $OC_6H_3F_2$), 6.87 (2 H, vt, *J* 8.6, *m*-H of $OC_6H_3F_2$), 2.20 (6 H, m, CH_2), 1.12 [9 H, dt, ^3J(PH) 17.6, ^3J(HH) 7.6, CH_3][g]

[a] Required values are given in parentheses. [b] Fast-atom bombardment with 3-nitrobenzyl alcohol as matrix. [c] Recorded in $CDCl_3$. [d] Crystallized with 0.33 CH_2Cl_2. [e] Crystallized with 0.5 CH_2Cl_2. [f] Repeated recrystallizations failed to give satisfactory analysis. [g] Recorded in $(CD_3)_2CO$.

decrease slightly in the order $P(OC_6H_3F_2\text{-}2,6)_3$ > **II** > **IV**. The values of δ_F for **II** and **IV** are similar to that for $P(OC_6H_3F_2\text{-}2,6)_3$ of δ −126.50.

Treatment of $[\{RhCl(\mu\text{-}Cl)(\eta^5\text{-}C_5Me_5)\}_2]$ with phosphonites **I** and **II** and phosphinites **III** and **IV** in refluxing benzene yielded $[RhCl_2L(\eta^5\text{-}C_5Me_5)]$ [L = $PPh(OPh)_2$ **1**, $PPh(OC_6H_3F_2\text{-}2,6)_2$ **2**, $PPh_2(OPh)$ **3** or $PPh_2(OC_6H_3F_2\text{-}2,6)$ **4**] as air-stable, red or orange microcrystalline solids (Scheme 2). The complexes were characterized by elemental analysis, mass, NMR and IR spectroscopies. The analytical, mass and ^{1}H NMR spectral data are given in Table 1, the ^{31}P-{^{1}H} and ^{19}F-{^{1}H} NMR data in Table 2. Complexes **1** and **4** have been further characterized by single-crystal X-ray diffraction studies.

Treatment of the dinuclear platinum complex $[\{PtCl(\mu\text{-}Cl)(PEt_3)\}_2]$ with the phosphonites **I** and **II** and the phosphinites **III** and **IV** in refluxing acetone yielded complexes of formulation $[PtCl_2(PEt_3)L]$ [L = $PPh(OPh)_2$ **5**, $PPh(OC_6H_3F_2\text{-}2,6)_2$ **6**, $PPh_2(OPh)$ **7** or $PPh_2(OC_6H_3F_2\text{-}2,6)$ **8**]. Complexes **5** and **7** occur exclusively as colourless *cis* isomers, whereas **6** and **8** occur as both *cis* and *trans* isomers. The pale yellow *trans* isomers **6a** and **8a** are formed initially, but isomerize in acetone solution over several days at room temperature to give the colourless *cis* isomers **6b** and **8b** (Scheme 2). It has also been found that *trans*-$[PtCl_2(PEt_3)\{P(OC_6H_3F_2\text{-}2,6)_3\}]$ isomerizes in acetone over several weeks.[13] It is thus apparent that the *cis* isomers are thermodynamically preferred for this series of complexes.

Table 2 The ^{31}P-{^{1}H} and ^{19}F-{^{1}H} NMR spectral data for $[RhCl_2L(\eta^5\text{-}C_5Me_5)]$ complexes[a]

L	δ_P	^1J(RhP)/Hz	δ_F	^4J(PF)/Hz
$P(OPh)_3$[b]	+104.2	240	—	—
$P(OC_6H_3F_2)_3$[b]	+111.5	239.5	−124.80	2.0
$PPh(OPh)_2$ (**1**)	+140.5	200	—	—
$PPh(OC_6H_3F_2)_2$ (**2**)	+151.0	205	−121.28	3.0
$PPh_2(OPh)$ (**3**)	+113.5	170.5	—	—
$PPh_2(OC_6H_3F_2)$ (**4**)	+128.0	173	−119.27	3.0
PPh_3[c]	+7.9	144	—	—

[a] Recorded in $CDCl_3$. [b] Ref. 12. [c] Ref. 17.

(No evidence for the formation of the *trans* isomers of **5** and **7** was obtained when the reactions between $[\{PtCl(\mu\text{-}Cl)(PEt_3)\}_2]$ and **I** and **III** were monitored by NMR spectroscopy.) The existence of *trans* isomers for the fluorine-containing ligands, but not for the perprotio ligands, is indicative of a significant steric influence exerted by the fluorine atoms in the *ortho* positions of the phenoxy rings. Complexes **5**–**8** were characterized by mass, NMR and IR spectroscopies. Elemental analyses were obtained for the *cis* complexes. The analytical, mass and ^{1}H NMR spectral data are presented in Table 1, the ^{19}F-{^{1}H} and ^{31}P-{^{1}H} NMR spectroscopic data in Table 3. The geometries of the compounds were determined from their ^{31}P-{^{1}H} NMR spectroscopic data and for complexes **6a**, **6b**, **7**, **8a**

Table 3 The ^{31}P-{^{1}H} and ^{19}F-{^{1}H} NMR spectral data for $[PtCl_2(PEt_3)L]$ complexes[a]

L	δ_P	^1J(PtP)/Hz	^2J(PP)/Hz	δ_F	^4J(PF)/Hz	^5J(PtF)/Hz
$P(OPh)_3$[b]	+62.7	6261	19	—	—	—
(*cis*)	(+16.5	3191)				
$P(OC_6H_3F_2)_3$[c,d]	+103.3	4126	713	−128.81	6.8	19.7
(*trans*)	(+17.8	2620)				
$P(OC_6H_3F_2)_3$[e,f]	+69.5	6389	19	−124.02	5.5	29.7
(*cis*)	(+17.3	3187)				
$PPh(OPh)_2$[e]	+93.8	5181	16	—	—	—
(*cis*) (**5**)	(+15.2	3348)				
$PPh(OC_6H_3F_2)_2$[c]	+136.8	3450	612	−125.06	6.0	15.7
(*trans*) (**6a**)	(+19.1	2517)				
$PPh(OC_6H_3F_2)_2$[c]	+111.2	5250	13	−123.09	4.6	24.1
(*cis*) (**6b**)	(+22.9	3280)				
$PPh(OC_6H_3F_2)_2$[e]	+106.6	5272	13	−123.41	4.2	19.2
(*cis*) (**6b**)	(+17.6	3307)				
$PPh_2(OPh)$[e]	+87.3	4362	16	—	—	—
(*cis*) (**7**)	(+12.6	3407)				
$PPh_2(OC_6H_3F_2)$[c]	+117.3	2837	522	−124.60	6.8	16.7
(*trans*) (**8a**)	(+19.5	2498)				
$PPh_2(OC_6H_3F_2)$[c]	+104.5	4450	15	−121.37	4.8	29.1
(*cis*) (**8b**)	(+19.8	3392)				

[a] Values for the PEt_3 ligand are given in parentheses. [b] Ref. 18. [c] Recorded in $(CD_3)_2CO$. [d] Ref. 12. [e] Recorded in $CDCl_3$. [f] Ref. 13.

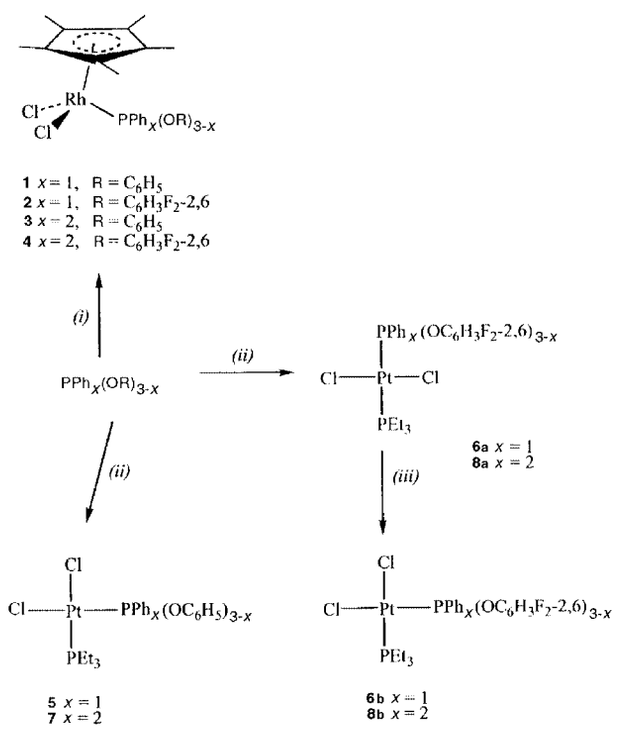

Scheme 2 (*i*) $[\{RhCl(\mu\text{-}Cl)(\eta^5\text{-}C_5Me_5)\}_2]$, C_6H_6, heat; (*ii*) $[\{PtCl(\mu\text{-}Cl)(PEt_3)\}_2]$, acetone, heat, 10 min; (*iii*) acetone, several weeks ($x = 1$) or days ($x = 2$)

and **8b** were confirmed by single-crystal X-ray diffraction studies.

Phosphorus-31 and ^{19}F NMR studies

The ^{31}P and ^{19}F NMR spectroscopic data for complexes **1**–**4** are given in Table 2, together with those for $[RhCl_2(PR_3)(\eta^5\text{-}C_5Me_5)]$ (R = OPh, $OC_6H_3F_2$-2,6 or Ph) for comparison. The ^{31}P-{^{1}H} NMR spectra exhibit doublet resonances. The values of δ_P for **1** and **2** are *ca.* 20 and 30 ppm respectively to higher frequency of those of the free phosphonites, whereas those for **3** and **4** are similar to those for **III** and **IV**. The values of δ_P thus show the same variation with the number of phenoxy groups as do those of the free phosphines. The values for **1** and **2** differ by *ca.* 10 ppm and those of **3** and **4** differ by *ca.* 15 ppm, with the resonances of those comprising the fluorine-containing ligands being at higher frequency than those of the respective perprotio analogue. The absolute values of the coupling constants ^1J(RhP) are intermediate between those for $[RhCl_2(PPh_3)(\eta^5\text{-}C_5Me_5)]$[17] and $[RhCl_2\{P(OC_6H_3F_2\text{-}2,6)_3\}(\eta^5\text{-}C_5Me_5)]$,[12] and follow the trend $[RhCl_2\{P(OC_6H_3F_2\text{-}2,6)_3\}(\eta^5\text{-}C_5Me_5)] \approx [RhCl_2\{P(OPh)_3\}(\eta^5\text{-}C_5Me_5)] > \mathbf{1} \approx \mathbf{2} > \mathbf{3} \approx \mathbf{4} > [RhCl_2(PPh_3)(\eta^5\text{-}C_5Me_5)]$. The order phosphite > phosphonite > phosphinite > phosphine is that anticipated from the greater electronegativity of the phenoxy group compared to that of the phenyl group.[16] Thus it appears that in the ^{31}P NMR spectrum the value ^1J(RhP) is indicative of the electronic nature of the phosphorus atom, whilst the value of δ_P is not. Furthermore, since the values of ^1J(RhP) for **1** and **2** and for **3** and **4** are very similar, substitution of hydrogen for fluorine in the *ortho* sites of the phenoxy rings of $PPh(OPh)_2$ and $PPh_2(OPh)$ does not significantly alter the electronic properties of the phosphorus in such complexes. The ^{19}F-{^{1}H} NMR spectra indicate that the values of δ_F, in contrast to those of δ_P, are sensitive to changes in the nature of the ligand and vary in a regular fashion, *i.e.* **2** and **4** exhibit doublets, which are shifted to higher frequency from those of the compounds **II** and **IV**, with that of **4** occurring at higher frequency than that of **2**, which, in turn, is at higher frequency than that of $[RhCl_2\{P(OC_6H_3F_2\text{-}2,6)_3\}(\eta^5\text{-}C_5Me_5)]$.[12] The values of ^4J(PF) are considerably smaller than those for the free phosphines, as is found for transition-metal complexes of $P(OC_6H_3F_2\text{-}2,6)_3$.[11–13] No rhodium–fluorine coupling is observed in the spectra. Presumably the values of ^5J(RhF) are too small to be resolved.

The ^{31}P and ^{19}F NMR data for complexes **5**–**8** are presented in Table 3, together with those for *cis*-$[PtCl_2(PEt_3)\{P(OPh)_3\}]$[18] and *cis*- and *trans*-$[PtCl_2(PEt_3)\{P(OC_6H_3F_2\text{-}2,6)_3\}]$[12,13] for comparison. A direct quantitative comparison of the NMR spectroscopic data cannot be made since the perprotio complexes are soluble in chloroform, but only sparingly so in acetone, whilst the fluorine-containing compounds are soluble in acetone, but virtually insoluble in chloroform. However, **6b** is sufficiently soluble in chloroform to allow the NMR spectra to be recorded, and the differences between the values of the chemical shifts and the coupling constants in the two solvents are small (Tables 1 and 3). In particular, δ_P is *ca.* 5 ppm to lower frequency and the magnitude of ^1J(PtP) is < 1% larger in chloroform than in acetone. Thus, the effects of the solvent on these values can be assumed to be small.

The value of δ_P for the phosphonite resonance of the *trans* complex **6a** is *ca.* 50 ppm to lower frequency of that of the free phosphonite **II**, whereas δ_P for the phosphinite resonance

of **8a** is only *ca.* 15 ppm to lower frequency of that of **IV**. The values for the PEt_3 resonance are similar, increasing slightly in the order *trans*-$[PtCl_2(PEt_3)\{P(OC_6H_3F_2\text{-}2,6)_3\}]$ > **6a** > **8a**. The absolute values of the phosphorus–phosphorus couplings, ^2J(PP), decrease regularly in the order *trans*-$[PtCl_2(PEt_3)\{P(OC_6H_3F_2\text{-}2,6)_3\}]$ > **6a** > **8a** from 713 Hz by *ca.* 100 Hz for each successive substitution of a $OC_6H_3F_2$-2,6 group for a phenyl group. The relatively high magnitudes are characteristic of *trans* complexes. The absolute values of the platinum–phosphorus couplings, ^1J(PtP), for the phosphite, phosphonite and phosphinite resonances also decrease regularly in the order *trans*-$[PtCl_2(PEt_3)\{P(OC_6H_3F_2\text{-}2,6)_3\}]$ > **6a** > **8a** from 4126 Hz by *ca.* 650 Hz for each successive substitution of a $OC_6H_3F_2$-2,6 group for a phenyl group. Absolute values for the Pt–PEt_3 coupling decrease in the same order, but by a smaller amount. The values of ^1J(PtP) are also consistent with *trans* complexes. The values of δ_F and ^4J(PF) are similar within the series, but the absolute values of ^5J(PtF) vary in the order *trans*-$[PtCl_2(PEt_3)\{P(OC_6H_3F_2\text{-}2,6)_3\}]$ > **8a** > **6a**.

The values of δ_P for the phosphite, phosphonite and phosphinite resonances for the *cis* complexes vary as those for the ligands and are at lower frequency than those of the *trans* complexes. For the PEt_3 resonance the values of δ_P show little variation between the complexes. The phosphorus–phosphorus couplings, ^2J(PP), have absolute values that are an order of magnitude lower than those of the respective *trans* complexes and show no discernible regular variation. The magnitude of the platinum–phosphorus coupling, ^1J(PtP), for the phosphite, phosphonite and phosphinite resonances decreases in the order *cis*-$[PtCl_2(PEt_3)\{P(OC_6H_3F_2\text{-}2,6)_3\}]$ [13] ≈ *cis*-$[PtCl_2(PEt_3)\{P(OPh)_3\}]$ [18] > **5** ≈ **6b** > **7** ≈ **8b** from 6389 by *ca.* 800 Hz on each successive substitution of a $OC_6H_3X_2$-2,6 (X = H or F) group for a phenyl group. The values for the fluorine-containing complexes are slightly larger than those for the respective perprotio analogues and are *ca.* 1800 Hz larger than for the respective *trans* complexes. The absolute values for the Pt–PEt_3 coupling are all between 3000 and 3500 Hz, and show no regular trend. The values of δ_F for the *cis* complexes are at higher frequency than those of the *trans* complexes by 2–4 ppm. The absolute values of ^4J(PF) are similar and are *ca.* 2 Hz smaller than those of the *trans* complexes. The absolute values of ^5J(PtF) vary in the order *cis*-$[PtCl_2(PEt_3)\{P(OC_6H_3F_2\text{-}2,6)_3\}]$ ≈ **8b** > **6b** and are *ca.* 10 Hz larger than those of the respective *trans* complexes. Thus ^1J(PtP) and ^5J(PtF) are larger for the *cis* complexes, whereas ^2J(PP) and ^4J(PF) are larger for the *trans* complexes. Within the series of *cis* and *trans* complexes two trends are observed in the coupling constants and chemical shifts: ^1J(PtP) and ^2J(PP) decrease regularly as $OC_6H_3X_2$ (X = H or F) groups are replaced by phenyl groups, whereas ^4J(PF) and ^5J(PtF) vary with the ligands $P(OC_6H_3F_2\text{-}2,6)_3$ ≈ **IV** > **II**, which is the inverse of the variation of δ_P. The variation in δ_P between the fluorine-containing complexes and their respective perprotio analogues is similar to that observed for the $[RhCl_2L(\eta^5\text{-}C_5Me_5)]$ complexes. The resonance for the fluorine-containing complex is shifted to higher frequency relative to that of the perprotio analogue, but the magnitude of the metal–phosphorus coupling constant is similar. The same trends in ^1J(PtP) are observed as in ^1J(RhP). Also, δ_F is shifted to higher frequency as $OC_6H_3X_2$ (X = H or F) groups are replaced by phenyl groups. It is evident that the magnitude of ^1J(MP) within the three series of complexes increases with increasing number of phenoxy groups. This is consistent with the magnitude of ^1J(MP) increasing with increasing electronegativity of the substituents on the phosphorus atom.[16] The similarity of ^1J(MP) for the perprotio complexes and their fluorine-containing analogues in the series $[RhCl_2L(\eta^5\text{-}C_5Me_5)]$ and *cis*-$[PtCl_2(PEt_3)L]$ shows that the presence of fluorine in the *ortho* positions of the phenoxy rings has a negligible electronic effect.

Table 4 Selected bond distances (Å) and angles (°) with estimated standard deviations (e.s.d.s) in parentheses about rhodium for $[RhCl_2L(\eta^5\text{-}C_5Me_5)]$ complexes [L = $PPh(OPh)_2$ **1** and $PPh_2(OC_6H_3F_2\text{-}2,6)$ **4**]*

	1		
	Molecule 1	Molecule 2	**4**
Rh–P	2.258(3)	2.254(3)	2.301(3)
Rh–Cl(1)	2.389(4)	2.378(3)	2.401(3)
Rh–Cl(2)	2.412(4)	2.391(4)	2.406(4)
Cp*–Rh	1.824(13)	1.822(15)	1.827(1)
Rh–C(1)	2.221(13)	2.251(14)	2.187(12)
Rh–C(2)	2.208(12)	2.206(13)	2.181(13)
Rh–C(3)	2.16(2)	2.147(14)	2.222(12)
Rh–C(4)	2.171(12)	2.15(2)	2.229(13)
Rh–C(5)	2.174(13)	2.15(2)	2.136(13)
P–Rh–Cl(1)	92.36(13)	92.57(12)	86.4(1)
P–Rh–Cl(2)	89.25(12)	90.99(13)	94.4(1)
Cl–Rh–Cl	89.6(2)	88.4(2)	92.3(1)
Cp*–Rh–P	129.1(4)	127.8(4)	130.85(10)
Cp*–Rh–Cl	121.7(4)	124.5(4)	124.2(1)
	123.9(4)	121.7(5)	118.5(1)

* Cp* denotes the cyclopentadienyl centroid.

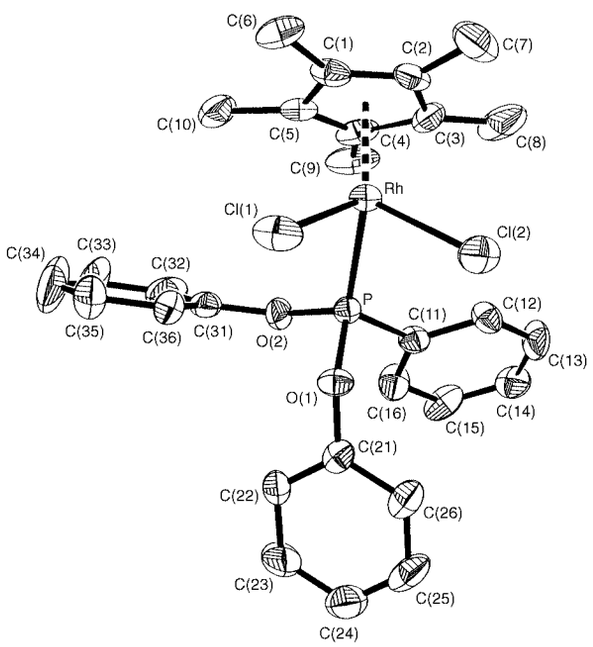

Fig. 1 Molecular structure of one of the independent molecules of $[RhCl_2\{PPh(OPh)_2\}(\eta^5\text{-}C_5Me_5)]$ **1**. Displacement ellipsoids are shown at the 30% probability level. The hydrogen atoms are omitted for clarity

Single-crystal X-ray diffraction studies

Selected bond distances and angles about the rhodium atom for complexes **1** and **4** are given in Table 4. Complex **1** crystallizes with two independent molecules in the unit cell, but the geometries of the two molecules are very similar. Both **1** (Fig. 1) and **4** (Fig. 2) display three-legged piano-stool geometries about the metal atom, similar to that of $[IrCl_2\{P(OC_6H_3F_2\text{-}2,6)_3\}(\eta^5\text{-}C_5Me_5)]$,[11] with the Cl–P–Cl and P–Rh–Cl angles being *ca.* 90°. The geometry of the ligands about the Cp*–Rh axis is distorted from pseudo-C_{3v} symmetry with the Cp*–Rh–P angles significantly greater than those of Cp*–Rh–Cl. The Cp*–Rh distances of the two molecules of **1** are the same within experimental error and are similar to that of **4**. The two molecules of **1** possess one shorter and one longer Rh–Cl bond, with those of one molecule being significantly longer than those of the other. The Rh–Cl bond lengths of **4** are the same within experimental error and comparable to those of **1**.

Table 5 Selected bond distances (Å) and angles (°) with e.s.d.s in parentheses about platinum for *trans*-[$PtCl_2(PEt_3)L$] [L = $P(OC_6H_3F_2\text{-}2,6)_3$, $PPh(OC_6H_3F_2\text{-}2,6)_2$ **6a** or $PPh_2(OC_6H_3F_2\text{-}2,6)$ **8a**]

		$PPh(OC_6H_3F_2\text{-}2,6)_2$ (**6a**)		
	L = $P(OC_6H_3F_2\text{-}2,6)_3$*	Molecule 1	Molecule 2	$PPh_2(OC_6H_3F_2\text{-}2,6)$ (**8a**)
Pt–$PPh_x(OR)_{3-x}$	2.243(2)	2.267(2)	2.267(4)	2.275(5)
Pt–PEt_3	2.304(3)	2.321(4)	2.319(4)	2.308(6)
Pt–Cl	2.296(2)	2.291(4)	2.285(4)	2.291(6)
	2.300(3)	2.310(4)	2.305(4)	2.312(6)
P–Pt–P	175.1(1)	177.2(1)	175.2(1)	176.1(2)
Cl–Pt–Cl	175.5(1)	175.3(1)	176.0(2)	177.5(2)
Cl–Pt–$PPh_x(OR)_{3-x}$	93.1(1)	90.7(1)	92.3(1)	92.0(2)
	87.8(1)	90.0(1)	87.7(1)	89.2(2)
Cl–Pt–PEt_3	89.6(1)	90.3(1)	91.0(1)	87.4(2)
	89.9(1)	88.8(1)	89.2(1)	91.6(2)

* Ref. 12.

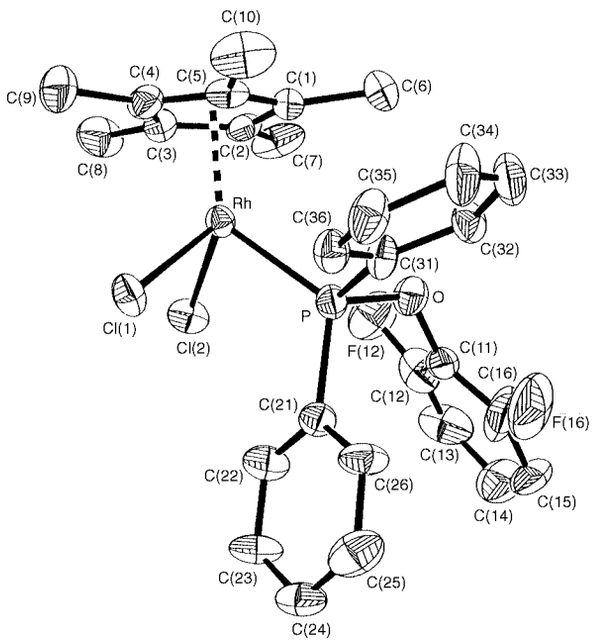

Fig. 2 Molecular structure of [$RhCl_2\{PPh_2(OC_6H_3F_2\text{-}2,6)\}(\eta^5\text{-}C_5Me_5)$] **4**. Details as in Fig. 1

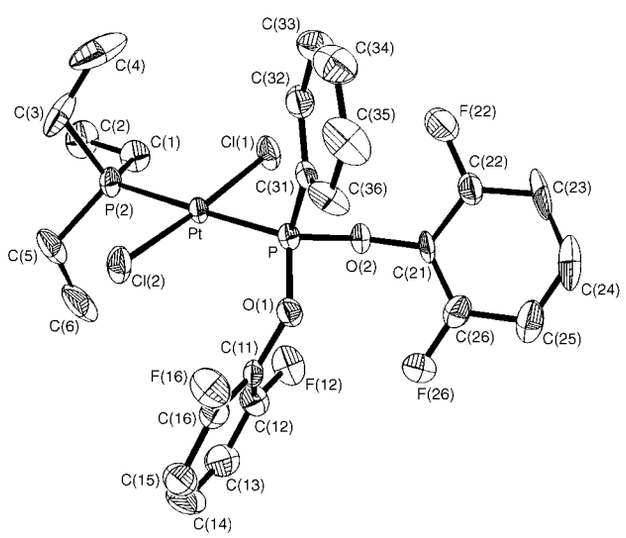

Fig. 3 Molecular structure of one of the independent molecules of *trans*-[$PtCl_2(PEt_3)\{PPh(OC_6H_3F_2\text{-}2,6\}_2$] **6a**. Details as in Fig. 1

The two independent molecules of complex **1** possess Rh–P bond lengths which are the same within experimental error, and are *ca.* 0.04 Å shorter than that of **4**. Three factors may be important in determining this distance. First, the electronic influence of the fluorine in the ligands. Values of ^1J(RhP) show this to be negligible, and comparison of the crystal structures of *cis*-[$PtCl_2(PEt_3)\{P(OPh)_3\}$][19] and *cis*-[$PtCl_2(PEt_3)\{P(OC_6H_3F_2\text{-}2,6)_3\}$][13] indicates that this has no effect upon the Pt–$P(OR)_3$ bond lengths. Secondly, the steric influence of the fluorine atoms, which would tend to increase the M–P distances for the complexes comprising fluorine-containing ligands. However, the similarity of the Pt–$P(OR)_3$ distances in *cis*-[$PtCl_2(PEt_3)\{P(OPh)_3\}$] and *cis*-[$PtCl_2(PEt_3)\{P(OC_6H_3F_2\text{-}2,6)_3\}$] suggests that steric differences in these ligands, induced by the presence of fluorine, is not dominant in determining the lengths of the Pt–P bonds. The structural data, therefore, suggest that the steric influence of the fluorine atoms has a small effect on M–P bond lengths. Thirdly, the π-bonding ability of the ligands. For phosphites this is greater than for phosphines and is manifested in shorter metal–phosphite bonds.[20] The π-bonding abilities of phosphonites and phosphinites are expected to be intermediate between those of phosphites and phosphines and follow the order $P(OR)_3 > PPh(OR)_2 > PPh_2(OR) > PPh_3$. The M–P bond lengths of **1** and **4** are consistent with this series, and it seems likely that it is this factor which dominates in determining the lengths of their Rh–P bonds. It is noted that the Rh–P bond distance of the rhodium complex **4** is *ca.* 0.04 Å longer than that of [$IrCl_2\{P(OC_6H_3F_2\text{-}2,6)_3\}(\eta^5\text{-}C_5Me_5)$],[11] which is consistent with the π-bonding ability of the ligands and further suggests that the steric influence of the fluorine atoms on the M–P bond lengths is not dominant. However, it should be noted that the Ir–P bonds are *ca.* 0.04 Å shorter than the Rh–P bonds in the complexes [$MCl\{(C_6F_5)_2PCH_2CH_2P(C_6F_5)_2\}(\eta^5\text{-}C_5Me_5)$]$^+BF_4^-$ (M = Rh or Ir).[10]

Selected bond distances and angles about platinum for the *trans* complexes **6a**, **8a** and, for comparison, [$PtCl_2(PEt_3)\{P(OC_6H_3F_2\text{-}2,6)_3\}$][12] are given in Table 5. (It should be noted that the crystal structure shows that *trans*-[$PtCl_2(PEt_3)\{P(OC_6H_3F_2\text{-}2,6)_3\}$] possesses short intermolecular H···F distances.) The structure of complex **6a** (Fig. 3) possesses two independent molecules in the unit cell; **8a** crystallizes with 0.75 molecules of water per molecule of complex (Fig. 4). The complexes possess square-planar geometries with X–Pt–X *trans* angles of 175.1(1)–177.5(2)° and P–Pt–Cl *cis* angles of 87.7(1)–93.1(1)°. The Pt–$PPh_x(OC_6H_3F_2\text{-}2,6)_{3-x}$ distances decrease in the order **8a** > **6a** > *trans*-[$PtCl_2(PEt_3)\{P(OC_6H_3F_2\text{-}2,6)_3\}$]. This is consistent with the π-bonding ability of the ligands. The Pt–PEt_3 distances do not show the reciprocal variation and decrease in the order **6a** > **8a** ≈ *trans*-[$PtCl_2(PEt_3)\{P(OC_6H_3F_2\text{-}2,6)_3\}$]. The complexes possess one Pt–Cl bond distance of *ca.* 2.30 Å or longer and one of less than 2.30 Å.

Selected bond distances and angles about platinum for the *cis*

Table 6 Selected bond distances (Å) and angles (°) with e.s.d.s in parentheses about platinum for *cis*-[$PtCl_2(PEt_3)L$] [L = $P(OPh)_3$, $P(OC_6H_3F_2\text{-}2,6)_3$, $PPh(OC_6H_3F_2\text{-}2,6)_2$ **6b**, $PPh_2(OPh)$ **7** or $PPh_2(OC_6H_3F_2\text{-}2,6)$ **8b**]

	L = $P(OPh)_3$ [a]	$P(OC_6H_3F_2\text{-}2,6)_3$ [b]	$PPh(OC_6H_3F_2\text{-}2,6)_2$ (**6b**)	$PPh_2(OPh)$ (**7**)	$PPh_2(OC_6H_3F_2\text{-}2,6)$ (**8b**)
Pt–$PPh_x(OR)_{3-x}$	2.182(2)	2.1772(14)	2.1819(13)	2.215(2)	2.2096(13)
Pt–PEt_3	2.269(1)	2.274(2)	2.271(2)	2.252(2)	2.2550(14)
Pt–Cl [*trans*-$PPh_x(OR)_{3-x}$]	2.344(2)	2.3248(14)	2.3488(14)	2.338(2)	2.343(2)
Pt–Cl (*trans*-PEt_3)	2.355(2)	2.3616(14)	2.346(2)	2.359(2)	2.3639(13)
P–Pt–P	97.9(1)	103.14(6)	102.05(5)	97.29(6)	97.57(5)
Cl–Pt–Cl	87.4(1)	88.61(5)	88.81(6)	87.58(6)	87.38(5)
Cl–Pt–$PPh_x(OR)_{3-x}$ (*trans*)	172.3(1)	171.52(5)	170.06(5)	170.14(6)	169.92(5)
(*cis*)	88.6(1)	83.66(5)	82.80(5)	83.02(6)	82.77(5)
Cl–Pt–PEt_3 (*trans*)	171.6(1)	172.16(5)	174.31(5)	177.50(6)	178.49(5)
(*cis*)	86.7(1)	84.61(6)	86.62(6)	92.33(6)	92.33(5)

[a] Ref. 19. [b] Ref. 13.

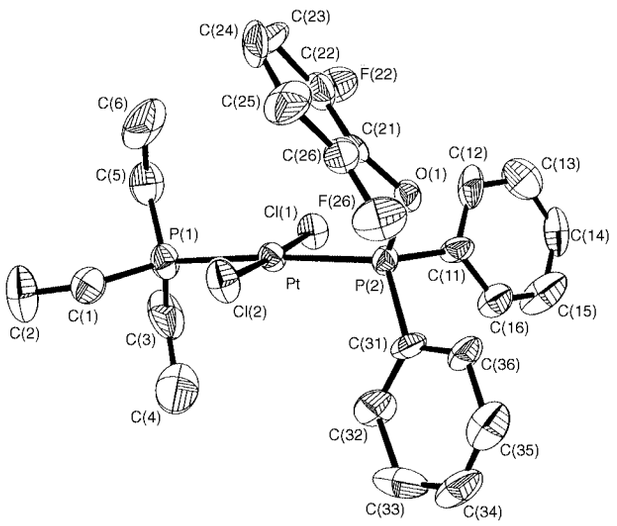

Fig. 4 Molecular structure of *trans*-[$PtCl_2(PEt_3)\{PPh_2(OC_6H_3F_2\text{-}2,6)\}$]·$0.75H_2O$ **8a**·$0.75H_2O$. Details as in Fig. 1

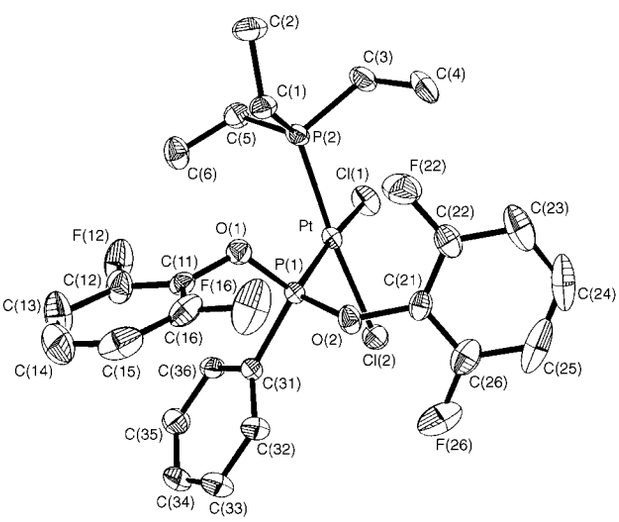

Fig. 5 Molecular structure of *cis*-[$PtCl_2(PEt_3)\{PPh(OC_6H_3F_2\text{-}2,6\}_2$] **6b**. Details as in Fig. 1

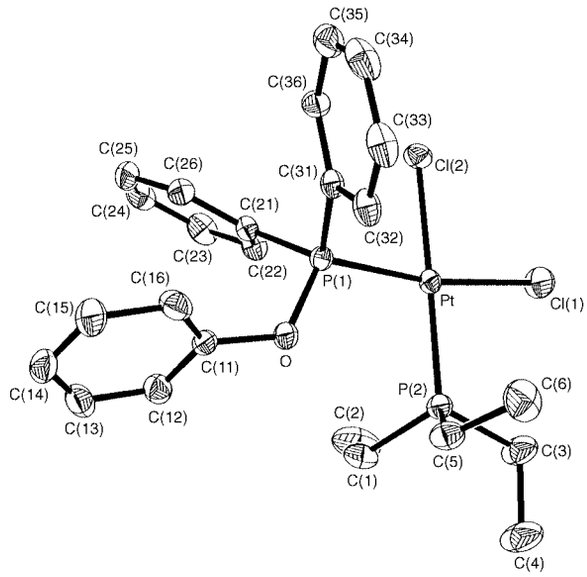

Fig. 6 Molecular structure of *cis*-[$PtCl_2(PEt_3)\{PPh_2(OPh)\}$] **7**. Details as in Fig. 1

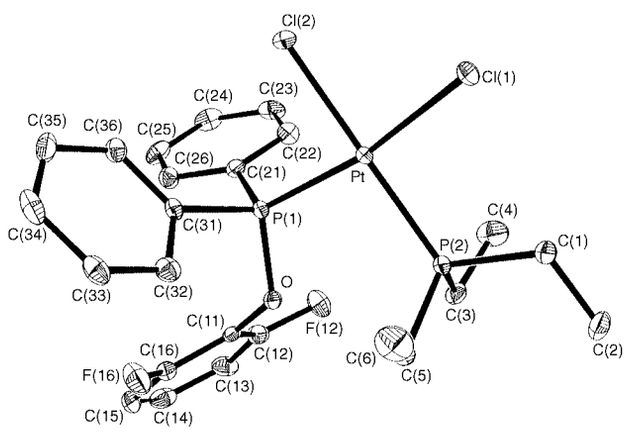

Fig. 7 Molecular structure of *cis*-[$PtCl_2(PEt_3)\{PPh_2(OC_6H_3F_2\text{-}2,6)\}$] **8b**. Details as in Fig. 1

complexes **6b**, **7**, **8b** and, for comparison, *cis*-[$PtCl_2(PEt_3)\{P(OC_6H_3F_2\text{-}2,6)_3\}$][13] and *cis*-[$PtCl_2(PEt_3)\{P(OPh)_3\}$][19] are given in Table 6 and the structures of **6b**, **7** and **8b** are shown in Figs. 5, 6 and 7 respectively. The Pt–Cl, Pt–P and P–O bond lengths of *cis*-[$PtCl_2(PEt_3)\{P(OC_6H_3F_2\text{-}2,6)_3\}$] and *cis*-[$PtCl_2(PEt_3)\{P(OPh)_3\}$] are within 0.01 Å of each other, and thus we may infer that the presence of fluorine in the *ortho* positions of the phenoxy groups has a negligible effect upon these distances. Thus, the Pt–Cl, Pt–P and P–O bond lengths of **7** may be compared directly with those of **6b** and *cis*-[$PtCl_2(PEt_3)\{P(OC_6H_3F_2\text{-}2,6)_3\}$]. The Pt–$PPh_x(OR)_{3-x}$ bond lengths decrease in the order **7** ≈ **8b** > **6b** ≈ *cis*-[$PtCl_2(PEt_3)\{P(OC_6H_3F_2\text{-}2,6)_3\}$] ≈ *cis*-[$PtCl_2(PEt_3)\{P(OPh)_3\}$] consistent with the trend observed for the *trans* complexes and the π-bonding ability of the ligands.

Table 7 Selected bond distances (Å) and bond and torsion angles (°) with e.s.d.s in parentheses for complexes of the phosphonites $PPh(OPh)_2$ (**1**) and $PPh(OC_6H_3F_2\text{-}2,6)_2$ (**6**)

	1		**6a**		
	Molecule 1	Molecule 2	Molecule 1	Molecule 2	**6b**
P–O(1)	1.608(9)	1.614(9)	1.612(9)	1.619(10)	1.616(4)
P–O(2)	1.623(9)	1.567(10)	1.621(8)	1.615(9)	1.607(4)
P–C	1.792(12)	1.837(12)	1.808(12)	1.782(13)	1.798(5)
O(1)–C	1.401(14)	1.399(14)	1.374(13)	1.362(15)	1.390(6)
O(2)–C	1.40(2)	1.40(2)	1.377(14)	1.381(16)	1.377(6)
C–CO(1)	1.35(2)	1.38(2)	1.368(17)	1.378(19)	1.354(8)
	1.38(2)	1.40(2)	1.376(18)	1.363(20)	1.374(8)
C–CO(2)	1.35(2)	1.34(2)	1.387(18)	1.465(27)	1.370(8)
	1.35(2)	1.39(2)	1.359(20)	1.321(29)	1.360(9)
C–F	—	—	1.341(17)	1.327(19)	1.356(7)
	—	—	1.346(15)	1.330(16)	1.329(8)
	—	—	1.375(18)	1.288(27)	1.352(8)
	—	—	1.325(16)	1.247(32)	1.337(8)
M–P–O(1)	112.1(3)	112.7(3)	119.4(3)	114.0(4)	115.0(2)
P–O(1)–C	123.6(8)	123.5(8)	128.1(7)	124.6(9)	124.3(3)
M–P–O(2)	117.2(3)	117.1(4)	112.0(3)	112.8(4)	117.54(1)
P–O(2)–C	129.7(9)	130.2(11)	123.8(7)	124.6(8)	126.0(3)
M–P–C	119.5(4)	116.4(4)	115.6(5)	119.4(5)	116.2(2)
O–P–O	104.7(5)	107.9(5)	103.5(4)	103.4(5)	101.3(2)
C–P–O(1)	104.6(5)	106.1(6)	98.7(5)	100.2(6)	103.2(2)
C–P–O(2)	96.7(5)	95.0(6)	105.0(5)	105.1(5)	101.6(2)
O(1)–C–C	122.5(12)	122.0(12)	125.4(11)	125.3(12)	120.0(5)
	117.0(13)	119.5(14)	117.8(10)	118.0(12)	122.5(5)
C–C[O(1)]–C	120.6(14)	118.4(13)	116.7(11)	116.6(12)	117.3(6)
O(2)–C–C	115(2)	112(2)	120.5(12)	116.0(14)	122.3(5)
	121(2)	125(2)	122.4(11)	123.5(17)	119.7(6)
C–C[O(2)]–C	124(2)	123(2)	116.8(12)	120.5(16)	117.7(6)
C(O)–C–F	—	—	117.5(12)	116.7(12)	117.4(5)
	—	—	119.0(11)	117.5(13)	118.2(6)
	—	—	116.6(12)	115.4(15)	117.0(6)
	—	—	119.7(12)	121.7(18)	118.3(7)
M–P–O–C	−168.8	171.8	24.3	−17.0	149.0
	−58.3	80.7	173.7	−154.5	3.1

The Pt–PEt_3 bond lengths increase in the order **7** ≈ **8b** < **6b** ≈ *cis*-$[PtCl_2(PEt_3)\{P(OC_6H_3F_2\text{-}2,6)_3\}]$ ≈ *cis*-$[PtCl_2(PEt_3)\{P(OPh)_3\}]$. The Pt–Cl bond lengths do not show a regular variation. For complexes **7**, **8b**, *cis*-$[PtCl_2(PEt_3)\{P(OC_6H_3F_2\text{-}2,6)_3\}]$ and *cis*-$[PtCl_2(PEt_3)\{P(OPh)_3\}]$ the Pt–Cl (*trans* to PEt_3) bond is significantly longer than Pt–Cl [*trans* to $PPh_x(OR)_{3-x}$], but for **6b** the two bond lengths are essentially identical. The P–O bond lengths decrease in the order **7** ≈ **6b** > *cis*-$[PtCl_2(PEt_3)\{P(OC_6H_3F_2\text{-}2,6)_3\}]$ ≈ *cis*-$[PtCl_2(PEt_3)\{P(OPh)_3\}]$ consistent with the P–O bond lengths in the *trans* complexes. The Pt–$PPh_x(OC_6H_3F_2\text{-}2,6)_{3-x}$ distances are considerably shorter for the *cis* than for the analogous *trans* complexes, consistent with triethylphosphine exerting a stronger *trans* influence than chloride.[18] The *trans* P–Pt–Cl angles lie in the range 169.92(5)–178.49(5)°. The values of Cl–Pt–Cl are similar for the complexes, lying in the range 87.38(5)–88.81(6)°. The P–Pt–P angles are, however, strongly affected by the presence of fluorine in the ligands. The P–Pt–P angle for *cis*-$[PtCl_2(PEt_3)\{P(OC_6H_3F_2\text{-}2,6)_3\}]$ is significantly larger than that of *cis*-$[PtCl_2(PEt_3)\{P(OPh)_3\}]$, which may be ascribed solely to the greater steric pressure of the fluorine atoms in $P(OC_6H_3F_2\text{-}2,6)_3$. The P–Pt–P angle of **6b** is similar to that of *cis*-$[PtCl_2(PEt_3)\{P(OC_6H_3F_2\text{-}2,6)_3\}]$ and that of **7** is similar to that of *cis*-$[PtCl_2(PEt_3)\{P(OPh)_3\}]$. The P–Pt–P angle of **8b** is, however, virtually identical to that of **7**, indicating that the steric influence of only two fluorine atoms on this angle is small.

Selected bond lengths and angles for the phosphonite ligands in complexes **1**, **6a** and **6b** are given in Table 7. The P–O distances for complexes are the same within experimental error, except for one considerably shorter distance in one of the unique molecules of **1**. The P–C distances lie in the range 1.782(13)–1.837(12) Å and the O–C distances lie in the range 1.362(15)–1.401(14) Å. The P–O–C angles for both the $[PtCl_2(PEt_3)\{PPh(OC_6H_3F_2\text{-}2,6)_2\}]$ complexes lie in the range 123.8(7)–128.1(7)°, whereas each unique molecule of **1** possesses one P–O–C angle of *ca.* 123.5° and another of *ca.* 130°. The M–P–O and M–P–C angles for all three complexes lie in the range 112.0(3)–119.5(4)°. Each unique molecule of **1** has an O–P–O and one O–P–C angle of *ca.* 105° and one O–P–C angle of *ca.* 96°. The two unique molecules of complex **6a** have O–P–O angles of *ca.* 103.5°, and each molecule has one O–P–C angle of *ca.* 99° and the other of *ca.* 105°. In contrast, the phosphonite ligand of **6b** shows pseudo-C_{3v} symmetry about the Pt–$PPh(OC_6H_3F_2\text{-}2,6)_2$ bond with Pt–P–X angles of *ca.* 116.5° and O–P–O and O–P–C angles of 101.3(2)–103.2(2)°. Thus it appears that the geometry of $[PtCl_2(PEt_3)\{PPh(OC_6H_3F_2\text{-}2,6)_2\}]$ does not greatly affect the bond distances within the phosphonite ligand, but does influence the angles about the phosphorus atom. It is interesting that the *cis* complex, which is the more sterically crowded of the two isomers, displays pseudo-C_{3v} symmetry about the Pt–$PPh(OC_6H_3F_2\text{-}2,6)_2$ bond, whilst the *trans* complex does not. Although there are similarities between some of the distances and angles in the phosphonite ligand of **1** and those of **6a** and **6b**, direct comparisons between the two ligands may not be valid because they are taken from non-analogous complexes. However, it is noted that the P–O–C and M–P–O angles for $PPh(OC_6H_3F_2\text{-}2,6)_2$ in complexes **6a** and **6b**, which are expected to be larger than those of $PPh(OPh)_2$ due to the steric influence of the bulky fluorine atoms, show no discernible increase over the values for **1**. All the complexes possess one M–P–O–C torsion angle with a magnitude of 150–180° and another with a magnitude of 0–90°.

Table 8 Selected bond distances (Å) and bond and torsion angles (°) with e.s.d.s in parentheses for complexes of the phosphinites $PPh_2(OPh)$ (**7**) and $PPh_2(OC_6H_3F_2\text{-}2,6)$ (**4**, **8**)

	7	**4**	**8a**	**8b**
P–O	1.630(4)	1.669(9)	1.636(14)	1.644(4)
P–C	1.812(6)	1.852(13)	1.809(24)	1.813(5)
	1.799(6)	1.814(14)	1.778(24)	1.812(5)
O–C	1.424(7)	1.407(16)	1.403(27)	1.401(6)
C–C(O)	1.364(9)	1.390(23)	1.379(35)	1.379(8)
	1.356(8)	1.381(27)	1.398(34)	1.371(8)
C–F	—	1.345(21)	1.369(50)	1.353(7)
	—	1.278(32)	1.333(31)	1.339(7)
M–P–O	113.2(2)	110.9(3)	115.8(6)	113.72(14)
P–O–C	124.0(4)	124.6(8)	125.0(13)	124.1(3)
M–P–C	115.2(2)	120.5(4)	120.9(8)	115.0(2)
	111.2(2)	111.8(4)	113.4(8)	110.8(2)
O–P–C	104.3(3)	105.4(5)	102.9(9)	104.1(2)
	103.8(2)	101.5(5)	98.7(9)	103.8(2)
C–P–C	108.3(3)	104.7(6)	102.5(11)	108.6(2)
O–C–C	117.7(5)	118.4(13)	122.5(21)	122.0(5)
	120.4(6)	118.6(17)	119.9(20)	120.6(5)
C–C(O)–C	121.8(6)	122.7(17)	117.5(22)	117.3(5)
C(O)–C–F	—	117.0(14)	117.4(22)	118.6(5)
	—	123.3(23)	117.3(21)	117.9(5)
M–P–O–C	−165.6	−120.1	14.3	−159.0

Selected bond lengths and angles for the phosphinite ligands in complexes **4**, **7**, **8a** and **8b** are given in Table 8. The P–O distances for the $[PtCl_2(PEt_3)L]$ complexes are similar at *ca.* 1.64 Å and the P–C distances lie in the range 1.778(24)–1.813(5) Å. The O–C distances for $PPh_2(OC_6H_3F_2\text{-}2,6)$ in complexes **8a** and **8b** are the same within experimental error, and the C–C (O) distances are similar, whereas the O–C distance in **7** is longer and the C–C (O) distance shorter than for the $PPh_2(OC_6H_3F_2\text{-}2,6)$ complexes. This is consistent with the difference displayed between $P(OPh)_3$[19] and $P(OC_6H_3F_2\text{-}2,6)_3$[13] in *cis*-$[PtCl_2(PEt_3)L]$. The P–O–C angles for the four complexes are all *ca.* 124–125°. The Pt–P–O, Pt–P–C, O–P–C and C–P–C angles for the *cis*-$[PtCl_2(PEt_3)L]$ complexes, **7** and **8b**, are very similar, consistent with the analogous data for *cis*-$[PtCl_2(PEt_3)\{P(OPh)_3\}]$ and *cis*-$[PtCl_2(PEt_3)\{P(OC_6H_3F_2\text{-}2,6)_3\}]$. This suggests that the presence of fluorine atoms in the phenoxy ring has virtually no steric effect within the ligand itself. The electron-withdrawing effect of the fluorine atoms does, however, manifest itself in shorter O–C distances. Complex **8a** possesses larger Pt–P–X angles and smaller O–P–C and C–P–C angles than the *cis* isomer, **8b**. All three $[PtCl_2(PEt_3)L]$ complexes show significant deviations from pseudo-C_{3v} symmetry about the Pt–$PPh_2(OR)$ bond. Complexes **4**, **7** and **8b** show *anti* arrangements of the M–P–O–C units with absolute torsion angles >120°, whereas **8a** possesses a *syn* arrangement of the Pt–P–O–C unit.

Within the series of $[PtCl_2(PEt_3)L]$ complexes the P–O distances decrease in the order $P(OPh)_3 \approx P(OC_6H_3F_2\text{-}2,6)_3 > PPh(OC_6H_3F_2\text{-}2,6)_2 > PPh_2(OPh) \approx PPh_2(OC_6H_3F_2\text{-}2,6)$. The P–C distances show no discernible trend, but the O–C distances decrease in the order $PPh_2(OPh) > PPh_2(OC_6H_3F_2\text{-}2,6) \approx P(OPh)_3 > P(OC_6H_3F_2\text{-}2,6)_3 > PPh(OC_6H_3F_2\text{-}2,6)_2$. The P–O–C angles are similar for all the $[PtCl_2(PEt_3)L]$.

Conclusion

The NMR and single-crystal X-ray diffraction studies of complexes of the type $[RhCl_2L(\eta^5\text{-}C_5Me_5)]$ and $[PtCl_2(PEt_3)L]$ indicate that substitution of hydrogen for fluorine in the *ortho* positions of phenoxy moieties in the phosphorus(III) ligands $PPh_x(OPh)_{3-x}$ ($x = 0$–2) produces a negligible electronic effect but a profound steric effect. Fluorophenyl groups are known to be considerably more electron-withdrawing than phenyl itself, as is demonstrated by the properties of pentafluorophenylphosphines and their metal complexes,[1–3] and thus the oxygen atom between the phosphorus atom and the phenyl ring is acting as an insulator. The oxygen atom also acts as a spacer removing the considerable steric pressure of the *o*-fluorine atoms away from the phosphorus and metal atoms, as is demonstrated by the similarity of the $Pt–PPh_x(OC_6H_3X_2\text{-}2,6)_{3-x}$ bond lengths for analogous perprotio and fluorine-containing complexes and the M–P bond distances being consistent with the order anticipated solely from the π-bonding abilities of the ligands. However, the greater size of the fluorine atom compared to that of the hydrogen atom still exerts a profound effect, as demonstrated by the formation of the *trans* platinum(II) complexes for the fluorine-containing ligands **II** and **IV**, but not for the perprotio ligands **I** and **III**, from their reactions with $[\{PtCl(\mu\text{-}Cl)(PEt_3)\}_2]$. The steric effect of the fluorine atoms can also greatly affect the angles about the metal, but has little effect upon the metal–phosphorus bond lengths.

Experimental

Physical measurements

The ^1H, ^{19}F and ^{31}P NMR spectra were recorded on a Bruker AM300 spectrometer at 300.14, 282.36 and 121.50 MHz respectively, ^1H referenced internally using the residual protio solvent resonance relative to tetramethylsilane (δ 0), ^{19}F externally to $CFCl_3$ (δ 0) and ^{31}P externally to 85% H_3PO_4 (δ 0). All chemical shifts are quoted in δ (ppm). Abbreviations used in multiplicities are s = singlet, d = doublet, t = triplet, q = quartet, qnt = quintet, m = multiplet and vt = virtual triplet. The IR spectra were recorded as neat oils or Nujol mulls between KBr plates on a Digilab FTS40 Fourier-transform spectrometer (s = strong, m = medium, w = weak). Elemental analyses were performed by Butterworth Laboratories Ltd. and mass spectra were recorded on a Kratos Concept 1H spectrometer.

Materials

The compounds $PPhCl_2$, PPh_2Cl, $[\{RhCl(\mu\text{-}Cl)(\eta^5\text{-}C_5Me_5)\}_2]$ (Aldrich) and 2,6-difluorophenol (Fluorochem) were used as supplied; $[\{PtCl(\mu\text{-}Cl)(PEt_3)\}_2]$ was prepared as described,[21] $PPh(OPh)_2$[14] and $PPh_2(OPh)$[15] as for $PPh(OMe)_2$.[22] Triethylamine was dried by storage over CaH_2, diethyl ether over sodium wire and then distilled from sodium–benzophenone under nitrogen. Unless stated otherwise, light petroleum of b.p. 40–60 °C was used.

Preparations

Bis(2,6-difluorophenyl) phenylphosphonite II. 2,6-Difluorophenol (17.49 g, 0.134 mol) and triethylamine (19 cm^3, 0.136 mol) in diethyl ether (80 cm^3) were added during 30 min to $PPhCl_2$ (6 cm^3, 0.045 mol) in diethyl ether (200 cm^3) at 0 °C. The white solid was filtered off and washed with diethyl ether (200 cm^3). The filtrate and washings were combined and the solvent removed under reduced pressure to give a pale yellow oil. The excess of triethylamine and 2,6-difluorophenol were distilled out at 60 °C and 0.4 mmHg (*ca.* 53 Pa) to yield the product as a yellow oil. No further attempts were made to purify compound **II** as it was found to be amenable to further reactions. Yield 7.73 g, 47%. $\delta_H(CDCl_3)$ 7.97 (2 H, m, PPh), 7.57 (3 H, m, PPh) and 6.95 (6 H, m, $OC_6H_3F_2$). $\delta_F(CDCl_3)$ −127.41 [d, ^4J(PF) 32.9 Hz]. $\delta_P(CDCl_3)$ 183.5 [qntm, ^4J(PF) 32.9, ^3J(PH) 7.1 Hz]. Electron impact (EI) mass spectrum: *m*/*z* 366 (M^+) and 237 ($[M - C_6H_3F_2]^+$) (Found: M^+, 366.04320. $C_{18}H_{11}F_4O_2P$ requires M^+, 366.04328). IR (neat): 3079w, 2961w, 2879w, 1601s, 1559w, 1503s, 1481s, 1440m, 1299s, 1247s, 1227s, 1209s, 1137w, 1111m, 1064m, 1013s, 924w, 870s, 781s, 749s, 693s, 637w, 578m, 501m and 430w cm^{-1}.

2,6-Difluorophenyl diphenylphosphinite IV. 2,6-Difluorophenol (13.90 g, 0.107 mol) and triethylamine (15 cm^3, 0.108 mol) in diethyl ether (80 cm^3) were added during 30 min to PPh_2Cl (15 cm^3, 0.084 mol) in diethyl ether (200 cm^3) at 0 °C. The white solid was filtered off and washed with diethyl ether (100 cm^3). The filtrate and washings were combined and the solvent removed under reduced pressure to give an orange oil. The excess of triethylamine and 2,6-difluorophenol were distilled out at 60 °C and 0.4 mmHg to yield the product as a yellow oil. No further attempts were made to purify compound **IV** as it was found to be amenable to further reactions. Yield 11.09 g, 41%. $\delta_H(CDCl_3)$ 7.66 (4 H, m, PPh), 7.45 (6 H, m, PPh) and 6.93 (3 H, m, $OC_6H_3F_2$). $\delta_F(CDCl_3)$ −126.69 [dtm, ^4J(PF) 28.5, ^3J(FH) 6.5 Hz]. $\delta_P(CDCl_3)$ 133.1 [tqntm, ^4J(PF) 28.5, ^3J(PH) 7.8 Hz]. EI mass spectrum: *m*/*z* 314 (M^+), 201 ($[M - C_6H_3F_2]^+$) and 185 ($[M - OC_6H_3F_2]^+$) (Found: M^+, 314.06723. $C_{18}H_{13}F_2OP$ requires M^+, 314.06721). IR (neat): 3073w, 3056w, 3008w, 1593m, 1559w, 1468s, 1476s, 1435s, 1386w, 1293s, 1244s, 1183w, 1130w, 1098m, 1059m, 1008s, 868s, 777s, 741s, 729s, 697s, 656w, 570w, 552w, 520m, 496m and 463w cm^{-1}.

$[RhCl_2\{PPh(OPh)_2\}(\eta^5\text{-}C_5Me_5)]$ 1. A slurry of $[\{RhCl(\mu\text{-}Cl)(\eta^5\text{-}C_5Me_5)\}_2]$ (0.202 g, 0.326 mmol) and $PPh(OPh)_2$ (0.210 g, 0.714 mmol) in benzene (50 cm^3) was heated under reflux under nitrogen for 3 h. The red solution was allowed to cool and the solvent removed by rotary evaporation to yield a red oil. The product was recrystallized from dichloromethane–light petroleum. Yield 0.168 g, 43%. IR (Nujol): 1590m, 1489m, 1438w, 1379w, 1212s, 1186s, 1157m, 1101m, 1077w, 1025m, 911 (sh), 900 (sh), 892s, 776m, 756m, 721m, 695m, 617w and 584m cm^{-1}.

$[RhCl_2\{PPh(OC_6H_3F_2\text{-}2,6)_2\}(\eta^5\text{-}C_5Me_5)]$ 2. A slurry of $[\{RhCl(\mu\text{-}Cl)(\eta^5\text{-}C_5Me_5)\}_2]$ (0.146 g, 0.237 mmol) and $PPh(OC_6H_3F_2\text{-}2,6)_2$ (0.190 g, 0.517 mmol) in benzene (50 cm^3) was heated under reflux under nitrogen for 2 h. The red solution was allowed to cool and concentrated by rotary evaporation to *ca.* 25 cm^3. Light petroleum (b.p. 100–120 °C, 120 cm^3) was added until the orange product, **2**, was precipitated. The solid was filtered off, washed with light petroleum (100 cm^3) and dried *in vacuo*. Yield 0.116 g, 36%. A sample for elemental analysis was recrystallized from dichloromethane–light petroleum. IR (Nujol): 1603w, 1509m, 1484s, 1312w, 1296m, 1248w, 1223w, 1198m, 1159w, 1103m, 1084w, 1063w, 1015s, 926s, 895s, 790w, 752m, 726m, 710w, 690m, 657w, 618w, 574m, 523m, 472w and 452m cm^{-1}.

$[RhCl_2\{PPh_2(OPh)\}(\eta^5\text{-}C_5Me_5)]$ 3. A slurry of $[\{RhCl(\mu\text{-}Cl)(\eta^5\text{-}C_5Me_5)\}_2]$ (0.210 g, 0.34 mmol) and $PPh_2(OPh)$ (0.203 g, 0.729 mmol) in benzene (60 cm^3) was heated under reflux under nitrogen for 2.5 h. The red solution was allowed to cool and concentrated by rotary evaporation to *ca.* 20 cm^3. Light petroleum (b.p. 100–120 °C, 100 cm^3) was added until the orange product, **3**, was precipitated. The solid was filtered off, washed with light petroleum (100 cm^3) and dried *in vacuo*. Yield 0.072 g, 38%. A sample for elemental analysis was recrystallized from dichloromethane–light petroleum. IR (Nujol): 1591m, 1489m, 1464m, 1437m, 1379m, 1216s, 1182w, 1157w, 1093m, 1078w, 915s, 752m, 726m, 696m, 614w, 578w, 564w, 521m and 496w cm^{-1}.

$[RhCl_2\{PPh_2(OC_6H_3F_2\text{-}2,6)\}(\eta^5\text{-}C_5Me_5)]$ 4. A slurry of $[\{RhCl(\mu\text{-}Cl)(\eta^5\text{-}C_5Me_5)\}_2]$ (0.106 g, 0.172 mmol) and $PPh_2(OC_6H_3F_2\text{-}2,6)$ (0.160 g, 0.511 mmol) in benzene (50 cm^3) was heated under reflux under nitrogen for 2 h. The red solution was allowed to cool and concentrated by rotary evaporation to *ca.* 25 cm^3. Light petroleum (b.p. 100–120 °C, 150 cm^3) was added until the orange product, **4**, was precipitated. The solid was filtered off, washed with light petroleum (100 cm^3) and dried *in vacuo*. Yield 0.182 g, 85%. IR (Nujol): 1599m, 1493s, 1478s, 1439m, 1378w, 1293m, 1243m, 1207s, 1181w, 1108m, 1084m, 1054w, 1028m, 1006s, 881s, 779m, 754m, 748s, 721s, 700m, 638w and 613w cm^{-1}.

***cis*-$[PtCl_2(PEt_3)\{PPh(OPh)_2\}]$ 5.** A slurry of $[\{PtCl(\mu\text{-}Cl)(PEt_3)\}_2]$ (0.111 g, 0.144 mmol) and $PPh(OPh)_2$ (0.109 g, 0.37 mmol) in acetone (40 cm^3) was heated to reflux for 10 min. The solution was allowed to cool and light petroleum (35 cm^3) was added. Concentration by rotary evaporation and further addition of light petroleum precipitated the product, which was recrystallized from dichloromethane–light petroleum. Yield 0.061 g, 31%. IR (Nujol): 1587m, 1484s, 1438m, 1377w, 1207m, 1183s, 1150m, 1114m, 1043m, 1018w, 924s, 808 (sh), 776s, 735m, 712m, 689m and 598m cm^{-1}.

***trans*- and *cis*-$[PtCl_2(PEt_3)\{PPh(OC_6H_3F_2\text{-}2,6)_2\}]$ 6a and 6b.** A slurry of $[\{PtCl(\mu\text{-}Cl)(PEt_3)\}_2]$ (0.100 g, 0.15 mmol) and $PPh(OC_6H_3F_2\text{-}2,6)_2$ (0.132 g, 0.15 mmol) in acetone (40 cm^3) was heated to reflux under nitrogen for 10 min to give a pale yellow solution. This was allowed to cool and concentrated by rotary evaporation. Addition of light petroleum (30 cm^3) precipitated the product as pale yellow crystals, which were filtered off, washed with light petroleum and dried *in vacuo*. Recrystallization from acetone–light petroleum yielded pale yellow crystals of the *trans* isomer, **6a**. Yield 0.072 g, 33%. IR (Nujol): 1653w, 1604w, 1558w, 1540w, 1496m, 1381s, 1299m, 1248w, 1219m, 1203m, 1153w, 1117w, 1060w, 1040w, 1012s, 933w, 916w, 895m, 839w, 774m (br), 760m (br), 729m, 692w, 668w, 576w, 526w, 481w and 458w cm^{-1} Over several weeks in acetone solution at room temperature isomerization of **6a** occurred to yield colourless crystals of *cis*-$[PtCl_2(PEt_3)\{PPh(OC_6H_3F_2\text{-}2,6)_2\}]$ **6b**. IR (Nujol): 1601m, 1559w, 1515s, 1481s, 1438m, 1415w, 1382w, 1304m, 1243m, 1219m, 1188s, 1115m, 1061m, 1038m, 1011s, 920s, 904s, 770s, 750m, 728s, 716m, 690m, 669w, 583m, 573w, 527w, 497w, 488w, 467w and 434w cm^{-1}.

$[PtCl_2(PEt_3)\{PPh_2(OPh)\}]$ 7. A slurry of $[\{PtCl(\mu\text{-}Cl)(PEt_3)\}_2]$ (0.159 g, 0.207 mmol) and $PPh_2(OPh)$ (0.159 g, 0.571 mmol) in acetone (40 cm^3) was heated to reflux under nitrogen for 10 min to give a pale yellow solution. The solution was allowed to cool and concentrated by rotary evaporation. Addition of light petroleum (35 cm^3) precipitated the product as colourless crystals, which were filtered off, washed with light petroleum and dried *in vacuo*. Recrystallization from acetone–light petroleum gave pale colourless crystals of complex **7**. Yield 0.093 g, 39%. IR (Nujol): 1559m, 1464s, 1437m, 1377m, 1188m, 1164m, 1105m, 1040m, 904w, 880s, 775m and 695m cm^{-1}.

***trans*- and *cis*-$[PtCl_2(PEt_3)\{PPh_2(OC_6H_3F_2\text{-}2,6)\}]$ 8a and 8b.** A slurry of $[\{PtCl(\mu\text{-}Cl)(PEt_3)\}_2]$ (0.100 g, 1.06 mmol) and $PPh_2(OC_6H_3F_2\text{-}2,6)$ (1.200 g, 3.82 mmol) in acetone (40 cm^3) was heated to reflux under nitrogen for 10 min to give a pale yellow solution. This was allowed to cool and concentrated by rotary evaporation to *ca.* 10 cm^3. Addition of light petroleum (50 cm^3) precipitated the product as pale yellow crystals, which were filtered off, washed with light petroleum and dried *in vacuo*. Recrystallization from acetone–light petroleum gave pale yellow crystals of the *trans* isomer, **8a**. Yield 0.129 g, 87%. IR (Nujol): 1539w, 1495m, 1467s, 1435m, 1379m, 1299m, 1243m, 1195m, 1152w, 1103s, 1036s, 1008s, 873s, 785m, 764m, 751s, 722s, 692s, 576m, 532m, 505w and 485w cm^{-1}. Over several days in acetone solution at room temperature isomerization of **8a** occurred to yield colourless crystals of *cis*-$[PtCl_2(PEt_3)\{PPh_2(OC_6H_3F_2\text{-}2,6)\}]$ **8b**. IR (Nujol): 1540w, 1493m, 1477m, 1435w, 1420w, 1383w, 1299m, 1241m, 1200s, 1151w, 1106s, 1040m, 1011s, 873s, 784m, 765w, 761s, 725m, 704w, 691m, 645w, 579m, 535m, 504w, 488w and 466w cm^{-1}.

Table 9 X-Ray crystal data collection, solution and refinement details[a] for $[RhCl_2\{PPh(OPh)_2\}(\eta^5\text{-}C_5Me_5)]$ **1**, $[RhCl_2\{PPh_2(OC_6H_3F_2\text{-}2,6)\}(\eta^5\text{-}C_5Me_5)]$ **4**, *trans*- and *cis*-$[PtCl_2(PEt_3)\{PPh(OC_6H_3F_2\text{-}2,6)_2\}]$ **6a** and **6b**, *cis*-$[PtCl_2(PEt_3)\{PPh_2(OPh)\}]$ **7**, *trans*-$[PtCl_2(PEt_3)\{PPh_2(OC_6H_3F_2\text{-}2,6)\}]\cdot 0.75H_2O$ **8a**·$0.75H_2O$ and *cis*-$[PtCl_2(PEt_3)\{PPh_2(OC_6H_3F_2\text{-}2,6)\}]$ **8b**

	1	**4**	**6a**	**6b**	**7**	**8a**	**8b**
Formula	$C_{28}H_{30}Cl_2O_2PRh$	$C_{28}H_{28}Cl_2F_2OPRh$	$C_{24}H_{26}Cl_2F_4O_2P_2Pt$	$C_{24}H_{26}Cl_2F_4O_2P_2Pt$	$C_{24}H_{30}Cl_2OP_2Pt$	$C_{24}H_{28}Cl_2F_2OP_2Pt\cdot 0.75H_2O$	$C_{24}H_{28}Cl_2F_2OP_2Pt$
M	603.30	623.30	750.38	750.38	662.41	714.4	698.39
T/K	293	293	293	293	293	293	190
Crystal size/mm	0.59 × 0.30 × 0.18	0.48 × 0.23 × 0.14	0.75 × 0.42 × 0.28	0.80 × 0.34 × 0.13	0.38 × 0.12 × 0.05	0.90 × 0.21 × 0.15	0.38 × 0.17 × 0.06
Crystal system	Orthorhombic	Monoclinic	Monoclinic	Monoclinic	Triclinic	Tetragonal	Triclinic
Space group	$P2_12_12_1$ [b]	$P2_1/c$	$P2_1/c$	$P2_1/c$	$P\bar{1}$	$P4_2/n$	$P\bar{1}$
a/Å	7.856(8)	15.416(5)	10.087(4)	8.335(1)	8.067(1)	23.719(2)	7.927(1)
b/Å	16.856(3)	10.069(3)	19.140(8)	15.561(2)	11.187(2)	—	10.811(1)
c/Å	41.244(4)	17.583(9)	29.597(15)	21.106(3)	15.087(2)	10.133(3)	15.432(4)
α/°	—	—	—	—	108.47(1)	—	105.72(2)
β/°	—	91.52(1)	97.01(4)	96.57(1)	91.11(1)	—	91.75(2)
γ/°	—	—	—	—	102.47(1)	—	100.34(2)
U/Å^3	5462(6)	2728(2)	5671(4)	2719.5(6)	1255.3(3)	5701(2)	1248.0(4)
Z	8 [c]	4	8 [c]	4	2	8	2
D_c/g cm^{-3}	1.467	1.517	1.758	1.833	1.753	1.665	1.859
μ/mm^{-1}	0.903	0.914	5.295	5.522	5.944	5.253	5.994
F(000)	2464	1264	2912	1456	648	2800	680
2θ Range/°	5.22–48.96	5.0–50.0	4.0–54.0	5.24–52.0	5.20–52.0	5.0–52.0	5.24–52.0
hkl Ranges	−1 to 8, −1 to 19, −1 to 48	−1 to 18, −1 to 12, −20 to 22	−1 to 12, −1 to 24, −37 to 37	−1 to 10, −1 to 19, −26 to 26	−1 to 9, −12 to 12, −18 to 18	−1 to 27, −1 to 27, −12 to 12	−1 to 9, −12 to 12, −19 to 19
Total data	6155	5735	13945	6936	5889	11 272	5565
Unique data (R_{int})	5866 (0.0622)	4602 (0.0524)	11 171 (0.0350)	5316 (0.0265)	4808 (0.0308)	5009 (0.0283)	4837 (0.0257)
Observed data [$I > 2\sigma(I)$]	4259	3092	6599	4010	3988	2204	4246
Least-squares variables	703	316	631	311	271	292	289
$R1$, $wR2$ [$I > 2\sigma(I)$] [d]	0.0563, 0.1182	0.0750, 0.1120	0.0563, 0.0711	0.0324, 0.0621	0.0360, 0.0706	0.0655, 0.0768	0.0316, 0.0719
(all data)	0.0937, 0.1406	0.1095, 0.1297	0.1029, 0.0892	0.0567, 0.0705	0.0528, 0.0763	0.1599, 0.1159	0.0408, 0.0765
Goodness of fit on F^2 [e]	1.055	1.69	0.91	1.031	1.011	1.06	1.026
Difference map features/e Å^{-3}	+0.918, −0.516	+1.96, −0.68	+1.36, −1.88	+0.607, −0.647	+0.838, −0.669	+2.19, −0.99	+0.946, −0.840
a,b in weighting scheme [f]	0.0499, 11.05	0.0674, 49.55	0.0343, 0	0.0228, 0.26	0.0246, 0	0.1135, 0	0.0347, 0.68

[a] Details in common: Siemens P4 diffractometer, λ(Mo-Kα) = 0.710 73 Å, ω-scan type, scan width 1.20. [b] Flack parameter 0.054 (0.068). [c] There are two independent molecules in the asymmetric unit. [d] $R1 = \Sigma||F_o| - |F_c||/\Sigma|F_o|$; $wR2 = [\Sigma w(F_o^2 - F_c^2)^2/\Sigma w(F_o^2)^2]^{\frac{1}{2}}$. [e] $S = \{\Sigma[w(F_o^2 - F_c^2)^2/(n-p)]\}^{\frac{1}{2}}$, where n = number of reflections and p the total number of parameters refined. [f] Weighting scheme, $w = 1/[\sigma^2(F_o^2) + (aP)^2 + bP]$ where $P = [\max(F_o^2, 0) + 2F_c^2]/3$.

X-Ray crystallography

Crystals suitable for single-crystal X-ray diffraction studies were grown from dichloromethane (complexes **1**, **4** and **7**) or acetone (**6a**, **6b**, **8a** and **8b**). Table 9 summarizes the crystallographic data. All data sets were corrected for Lorentz-polarization effects and absorption corrections were applied based on ψ-scan data. The structures were solved by Patterson methods using the program SHELXTL-PC[23] and refined on F^2 using full-matrix least squares; **4**, **6a** and **8a** were refined using the program SHELXTL-PC and **1**, **6b**, **7** and **8b** using SHELXL 93.[24] There were two crystallographically unique molecules in the asymmetric units of both **1** and **6a**. The absolute configuration was determined for **1** with the Flack parameter 0.054 (0.068). All non-hydrogen atoms were refined as anisotropic with the exception of the solvent atoms in **8a**. High values for anisotropic displacement parameters of some atoms were found for **1**, **6a** and **7**. Attempts to account for these in terms of disordered models did not lead to significant improvements in the refinements.

Atomic coordinates, thermal parameters, and bond lengths and angles have been deposited at the Cambridge Crystallographic Data Centre (CCDC). See Instructions for Authors, *J. Chem. Soc.*, *Dalton Trans.*, 1997, Issue 1. Any request to the CCDC for this material should quote the full literature citation and the reference number 186/373.

Acknowledgements

We thank BNFL Fluorochemicals Ltd. (to G. C. S.) and the Royal Society (to E. G. H.) for support and K. S. Coleman for helpful discussion.

References

1 R. D. W. Kemmitt, D. I. Nichols and R. D. Peacock, *Chem. Commun.*, 1967, 599; R. D. W. Kemmitt, D. I. Nichols and R. D. Peacock, *J. Chem. Soc. A*, 1968, 1898, 2149.
2 M. J. Atherton, K. S. Coleman, J. Fawcett, J. H. Holloway, E. G. Hope, A. Karaçar, L. A. Peck and G. C. Saunders, *J. Chem. Soc.*, *Dalton Trans.*, 1995, 4029.
3 J. H. Holloway, E. G. Hope, D. R. Russell, G. C. Saunders and M. J. Atherton, *Polyhedron*, 1996, **15**, 173.
4 J. H. Holloway, E. G. Hope, G. C. Saunders and A. M. Stuart, unpublished work.
5 I. Ojima and H. B. Kwon, *J. Am. Chem. Soc.*, 1988, **110**, 5617.
6 M. F. Ernst and D. M. Roddick, *Inorg. Chem.*, 1990, **29**, 3627.
7 R. K. Merwin, R. C. Schnabel, J. D. Koola and D. M. Roddick, *Organometallics*, 1992, **11**, 2972.
8 M. J. Atherton, J. Fawcett, J. H. Holloway, E. G. Hope, A. Karaçar, D. R. Russell and G. C. Saunders, *J. Chem. Soc.*, *Chem. Commun.*, 1995, 191.
9 A. S. Chan, C.-C. Pai, T.-K. Yang and S.-M. Chen, *J. Chem. Soc.*, *Chem. Commun.*, 1995, 2031.
10 M. J. Atherton, J. Fawcett, J. H. Holloway, E. G. Hope, A. Karaçar, D. R. Russell and G. C. Saunders, *J. Chem. Soc.*, *Dalton Trans.*, 1996, 3215.
11 J. H. Holloway, E. G. Hope, K. Jones, G. C. Saunders, J. Fawcett, N. Reeves, D. R. Russell and M. J. Atherton, *Polyhedron*, 1993, **12**, 2681.
12 K. S. Coleman, J. H. Holloway, E. G. Hope, D. R. Russell, G. C. Saunders and M. J. Atherton, *Polyhedron*, 1995, **14**, 2107.
13 J. Fawcett, J. H. Holloway, E. G. Hope, G. C. Saunders and M. J. Atherton, *Acta Crystallogr.*, *Sect. C*, 1996, **52**, 2463.
14 K. A. Petrov, V. P. Evdakov, K. A. Bilevich and Y. S. Kosarev, *Zh. Obshch. Khim.*, 1962, **32**, 1974.
15 M. Sander, *Chem. Ber.*, 1960, **93**, 1220.
16 P. S. Pregosin and R. W. Kunz, *NMR 16, Basic Principles and Progress*, Springer, Berlin, 1979.
17 J. H. Holloway, E. G. Hope and G. C. Saunders, unpublished work.
18 F. H. Allen and S. N. Sze, *J. Chem. Soc. A*, 1971, 2054.
19 A. N. Caldwell, L. Manojlović-Muir and K. W. Muir, *J. Chem. Soc.*, *Dalton Trans.*, 1977, 2265.
20 A. D. U. Hardy and G. A. Sim, *J. Chem. Soc.*, *Dalton Trans.*, 1972, 1900.
21 R. J. Goodfellow and L. M. Venanzi, *J. Chem. Soc.*, 1965, 7533.
22 K. S. Colle and E. S. Lewis, *J. Org. Chem.*, 1978, **43**, 571.
23 G. M. Sheldrick, SHELXTL-PC, Release 4.2, Siemens Analytical X-Ray Instruments, Madison, WI, 1991.
24 G. M. Sheldrick, SHELXL 93, Program for Crystal Structure Refinement, University of Göttingen, 1993.

Received 25*th September* 1996; *Paper* 6/06584H